



Synthesis and preliminary structure-activity relationship study of 3-methylquinazolinone derivatives as EGFR inhibitors with enhanced antiproliferative activities against tumour cells

Yan Zhang^{a,b,c}, Qin Wang^{a,b,c}, Luolan Li^{b,d}, Yi Le^{a,b,c}, Li Liu^{a,c}, Jing Yang^a, Yongliang Li^e, Guochen Bao^f  and Longjia Yan^{a,b,c} 

^aSchool of Pharmaceutical Sciences, Guizhou University, Guiyang, China; ^bState Key Laboratory of Functions and Applications of Medicinal Plants, Guizhou Medical University, Guiyang, China; ^cGuizhou Engineering Laboratory for Synthetic Drugs, Guiyang, China; ^dShizhen College of Guizhou University of Traditional Chinese Medicine, Guiyang, China; ^eFaculty of Light Industry and Chemical Engineering, Guangdong University of Technology, Guangzhou, China; ^fInstitute for Biomedical Materials and Devices (IBMD), Faculty of Science, University of Technology Sydney, Sydney, Australia

ABSTRACT

In this paper, a set of 3-methylquinazolinone derivatives were designed, synthesised, and studied the preliminary structure-activity relationship for antiproliferative activities. All target compounds performed significantly inhibitory effects against wild type epidermal growth factor receptor tyrosine kinase (EGFR^{WT}-TK) and tumour cells (A431, A549, MCF-7, and NCI-H1975). In particular, compound **4d** 3-fluoro-*N*-(4-((3-methyl-4-oxo-3,4-dihydroquinazolin-2-yl)methoxy)phenyl)benzamide showed higher antiproliferative activities against all tumour cells than Gefitinib (IC₅₀ of 3.48, 2.55, 0.87 and 6.42 μM, respectively). Furthermore, compound **4d** could induce apoptosis of MCF-7 cells and arrest in G2/M phase at the tested concentration. Molecular docking and ADMET studies showed that compound **4d** could closely form many hydrogen bonds with EGFR^{WT}-TK. Therefore, compound **4d** is potential to develop as novel anti-cancer drug.

ARTICLE HISTORY

Received 28 April 2021
Revised 15 May 2021
Accepted 17 May 2021

KEYWORDS

Quinazolinone; EGFR; kinase inhibitor; structure-activity relationship; antiproliferative

1. Introduction

Epidermal growth factor receptor (EGFR) tyrosine kinase (TK), a receptor tyrosine kinase, plays an important role in the process of survival, proliferation, angiogenesis, tumour micro environment, and adhesion of several malignant tumors¹. Overexpression or mutation of EGFR has been observed in many human tumour cells, such as non-small-cell lung cancer (NSCLC), breast cancer, and brain cancer². Due to its crucial status related to cancer development, EGFR has been considered a potential drug target for many years^{3–5}. Currently, a series of EGFR inhibitors were developed and approved into clinical phases, such as Gefitinib, Erlotinib, Icotinib, Afatinib, and Osimertinib⁶. However, with the continuous emergence of drug resistance in EGFR inhibitors in clinic, design and synthesis of novel EGFR inhibitors have become an urgent work for anti-tumour drug discovery⁷.






Quinazolinone is the main skeleton of many natural products^{8,9}, for example Allicin C, Cyclosporin F, Rutaecarpine, and (+)-Changshanine (Figure 1). These compounds have a wide range of biological activities, including antitumor, antibacterial, antiviral, and anti-inflammatory^{10–12}. Therefore, many groups have developed new methods to synthesise quinazolinone derivatives¹³. Patel et al. reported 2-phenylquinazolinone derivatives as EGFR inhibitors in 2017¹⁴ and recently inspired from natural alkaloid L-norephedrine, Ghorab et al. published a 3-substituted quinazolinones for


EGFR inhibitors¹⁵. These results indicate that the development of novel quinazolinone EGFR inhibitors has attracted extensive attentions.

Our group has been focussed on the research of developing new anti-tumour drugs for several years^{16–19}. We have synthesised lots of antiproliferative compounds such as benzodiazepines, 1,3,4-oxadiazoles, 1,3,4-thiadiazoles²⁰, and pyrimidines²¹. Based on the broad activities of quinazolinone and imperative need for EGFR inhibitors, we reported a series of 3-methylquinazolinone derivatives for EGFR inhibitors in last year²². As shown in Figure 1, the IC₅₀ value of compound **A** against EGFR^{WT} reached to 47 nm. However, further studies showed that compound **A** was not stable in mice plasma (Figure S1). The result prompted us to seek more valuable 3-methylquinazolinone derivatives. To overcome the metabolic stability in our previous research, we herein describe the design, synthesis, and studies the preliminary structure-activity relationship (SAR) of new 3-methylquinazolinone derivatives as EGFR inhibitors.

2. Experimental section

All reagents were commercially available in Sigma-Aldrich with analytical purity. Melting points were tested in digital melting point analyser with micro-display window (uncorrected, Shanghai

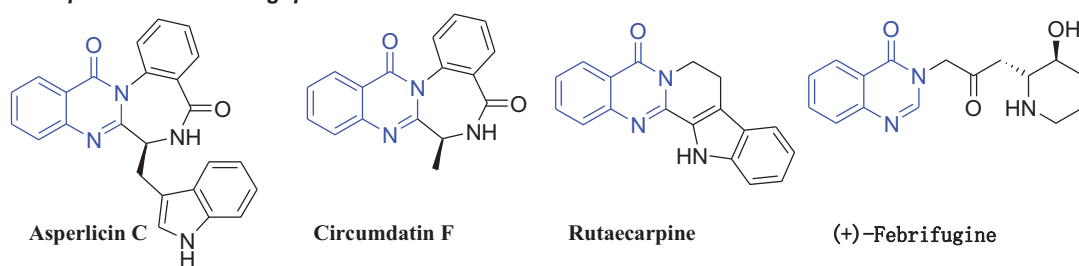
CONTACT Yi Le  yile2021@163.com  School of Pharmaceutical Sciences, Guizhou University, Guiyang 550025, China; Yongliang Li  yongliangli@gdut.edu.cn  Faculty of Light Industry and Chemical Engineering, Guangdong University of Technology, Guangzhou 510006, China; Longjia Yan  yjl1089@163.com School of Pharmaceutical Sciences, Guizhou University, Guiyang 550025, China

 Supplemental data for this article can be accessed [here](#).

© 2021 The Author(s). Published by Informa UK Limited, trading as Taylor & Francis Group.

This is an Open Access article distributed under the terms of the Creative Commons Attribution License (<http://creativecommons.org/licenses/by/4.0/>), which permits unrestricted use, distribution, and reproduction in any medium, provided the original work is properly cited.

Nature products containing quinazolinone:



Our Strategy:

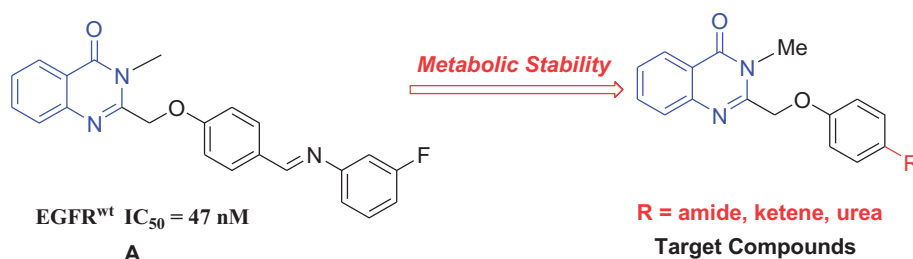


Figure 1. Natural products of quinazolinone and our strategy.

Microelectronics Technology Co. Ltd.). The ¹H and ¹³C NMR spectra were recorded on Bruker (Avance) 400 MHz and JEOL (Japan) 500 MHz NMR instrument with chemical reported as δ in CDCl₃ and DMSO-d₆, tetramethylsilane (TMS) as the internal standard. The high-resolution mass spectrometer (HRMS) was tested in TSQ 8000 high-resolution mass spectrometer and AB SCIEX X500R QTOF.

2.1. Synthesis

The synthetic route of compounds **4a–4g** was shown in Scheme 1. The experimental methods and details were described as follows.

2.1.1. 2-(Chloromethyl)-3-methylquinazolin-4(3H)-one (**2**)

2-Amino-*N*-methylbenzamide (1.5 g, 10 mmol) was dissolved in acetic acid (50 ml), and then 2-chloroacetyl chloride (3.36 g, 30 mmol) was added. The mixture was stirred for 6 h under refluxing. Then, the solution was evaporated *in vacuo* and neutralised with aqueous NaHCO₃. The crude product was filtered and purified with recrystallisation from ethanol. The product was dried in vacuum to give a white solid. 1.04 g; 50% yield; ¹H NMR (400 MHz, CDCl₃) δ 8.29 (d, *J* = 8.0 Hz, 1H), 7.80–7.75 (m, 1H), 7.68–7.69 (m, 1H), 7.50–7.54 (m, 1H), 4.65 (s, 2H), 3.76 (s, 3H). Spectral properties were in accordance with the literature²³.

2.1.2. 4-((3-Methyl-4-oxo-3,4-dihydroquinazolin-2-yl)methoxy)benzaldehyde (**3**)

p-Hydroxybenzaldehyde (610 mg, 5 mmol) was dissolved in DMF (20 ml), and then anhydrous K₂CO₃ (759 mg, 5.5 mmol) was added. After stirred for 15 min at room temperature, the mixture was added compound **2** (1.04 g, 5 mmol) and KI (913 mg, 5.5 mmol). The solution was stirred for the other 2 h, and poured into water (40 ml). The crude product was filtered and purified with recrystallisation from ethanol. The product was dried in vacuum to give a light-yellow solid. 1 g; 68% yield; ¹H NMR (DMSO, 400 MHz), δ 9.90 (s, 1H), 8.16 (dd, *J* = 8.0, 1.0 Hz, 1H), 7.90 (d, *J* = 8.8 Hz, 2H), 7.82 (ddd, *J* = 8.4, 7.2, 1.6 Hz, 1H), 7.63 (d, *J* = 7.6 Hz, 1H), 7.60–7.52 (m,

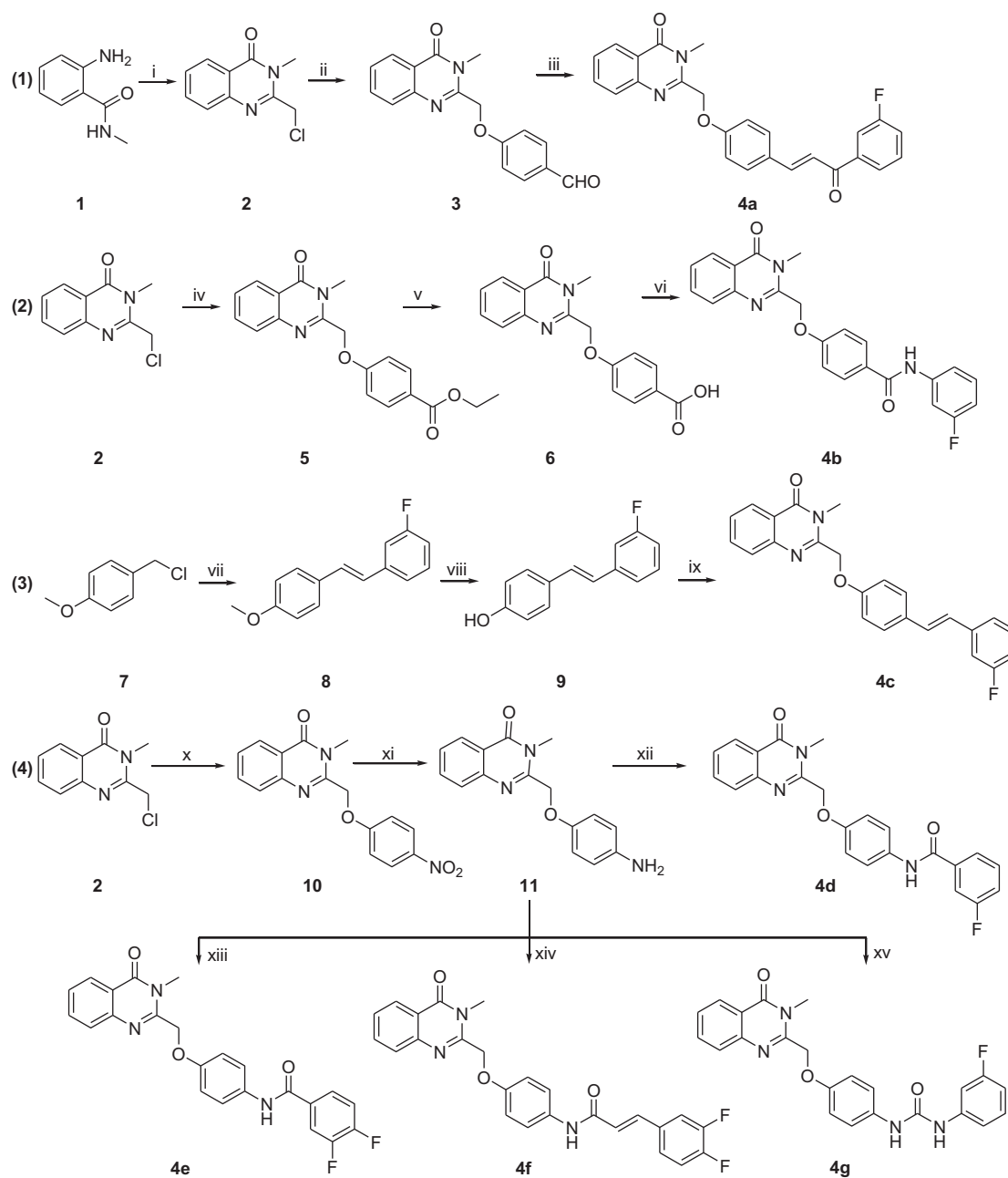
1H), 7.32 (d, *J* = 8.8 Hz, 2H), 5.45 (s, 2H), 3.62 (s, 3H). Spectral properties were in accordance with the literature²³.

2.1.3. (E)-2-((4-(3-(3-Fluorophenyl)-3-oxoprop-1-enyl)phenoxy)-methyl)-3-methylquinazolin-4(3H)-one (**4a**)

1-(3-Fluorophenyl)ethanone (276 mg, 2 mmol) and 4-((3-methyl-4-oxo-3,4-dihydroquinazolin-2-yl)methoxy)benzaldehyde (588 mg, 2 mmol) were dissolved in EtOH (20 ml), and then 2 mol/l NaOH (1 ml) was added. The mixture was stirred for 6 h at room temperature. Then, the solution was neutralised with 2 mol/l HCl (1 ml). The crude product was filtered and purified by chromatography using PE/EtOAc = 1/1 as the fluent solvent. The product was dried in vacuum to give a white solid. 348 mg; 42% yield; m.p. 208–209 °C; ¹H NMR (400 MHz, DMSO) δ 8.17 (d, *J* = 7.6 Hz, 1H), 8.02–7.75 (m, 7H), 7.67–7.52 (m, 4H), 7.22 (d, *J* = 8.4 Hz, 2H), 5.40 (s, 2H), 3.63 (s, 3H); ¹³C NMR (125 MHz, DMSO) δ 189.5, 161.8, 161.6, 160.5, 159.6, 152.7, 146.9, 145.1, 135.0, 134.5 (d, *J* = 8.5 Hz), 131.3, 130.9 (d, *J* = 3.0 Hz, 7H), 128.2, 127.9, 127.7, 126.8, 125.3 (d, *J* = 3.5 Hz), 124.2 (d, *J* = 3.5 Hz), 120.8, 117.1 (d, *J* = 22.0 Hz), 116.1, 69.0, 30.4; HRMS-ESI (*m/z*): [M + H]⁺ calcd for C₂₅H₁₉FN₂O₃, 415.1452; found, 415.1452.

2.1.4. Ethyl 4-((3-methyl-4-oxo-3,4-dihydroquinazolin-2-yl)methoxy)benzoate (**5**)

Ethyl 4-hydroxybenzoate (830 mg, 5 mmol) was dissolved in DMF (20 ml), and then anhydrous K₂CO₃ (759 mg, 5.5 mmol) was added. After stirred for 15 min at room temperature, the mixture was added compound **2** (1.04 g, 5 mmol) and KI (913 mg, 5.5 mmol). The solution was stirred for the other 2 h, and poured into water (40 ml). The crude product was filtered and purified with recrystallisation from ethanol. The product was dried in vacuum to give a white solid. 1.08 g; 64% yield; m.p. 114–116 °C; ¹H NMR (400 MHz, CDCl₃) δ 8.30 (d, *J* = 8.8 Hz, 1H), 8.03 (d, *J* = 8.8 Hz, 2H), 7.77 (t, *J* = 7.6 Hz, 1H), 7.71 (d, *J* = 7.6 Hz, 1H), 7.52 (t, *J* = 8.0 Hz, 1H), 7.10 (d, *J* = 8.8 Hz, 2H), 5.25 (s, 2H), 4.35 (q, *J* = 7.2 Hz, 2H), 3.74 (s, 3H), 1.38 (t, *J* = 7.2 Hz, 3H); ¹³C NMR (100 MHz, DMSO) δ 165.7, 162.0, 161.7, 152.5, 146.9, 134.9, 131.6, 127.8, 127.6, 126.7, 123.4, 120.7,



Scheme 1. Synthetic route of compounds **4a-4g**. Reagents and conditions: i) 2-chloroacetyl chloride, AcOH, reflux, 50% yield; ii) 4-hydroxybenzaldehyde, K_2CO_3 , KI, DMF, rt, 68% yield; iii) 3-fluorophenylethanone, NaOH, EtOH, rt, 42% yield; iv) ethyl 4-hydroxybenzoate, K_2CO_3 , KI, DMF, rt, 64% yield; v) NaOH, EtOH, rt, 58% yield; vi) 3-fluorobenzamide, HATU, DIEA, DMF, rt, 38% yield; vii) triethyl phosphite, tetrabutylammonium bromide, 130 °C, then 3-fluorobenzaldehyde, NaH, THF, rt, 43% yield; viii) BBr_3 , DCM, 0–10 °C, 72% yield; ix) compound **2**, K_2CO_3 , KI, DMF, rt, 47% yield; x) 4-nitrophenol, K_2CO_3 , KI, DMF, rt, 53% yield; xi) Pd/C, MeOH, H_2 , rt, 72% yield; xii–xv) corresponding acid or isocyanate, HATU, DIEA, DMF, rt, 30–37% yield.

115.5, 68.8, 60.9, 30.3, 14.7; HRMS-ESI (m/z): $[M + H]^+$ calcd for $C_{19}H_{18}N_2O_4$, 339.1339; found, 339.1339.

2.1.5. 4-((3-Methyl-4-oxo-3,4-dihydroquinazolin-2-yl)methoxy)benzoic acid (**6**)

Compound **5** (676 mg, 2 mmol) was dissolved in EtOH (10 ml), and then 2 mol/l NaOH (2 ml) was added. The mixture was stirred for 6 h at room temperature. Then, the solution was neutralised with 2 mol/l HCl (2 ml). The crude product was filtered and dried in vacuum to give a white solid. 360 mg; 58% yield; m.p. 97–99 °C; 1H NMR (400 MHz, DMSO) δ 12.69 (s, 1H), 8.16 (d, $J = 7.6$ Hz, 1H), 7.91 (d, $J = 8.8$ Hz, 2H), 7.83 (t, $J = 8.0$ Hz, 1H), 7.65 (d, $J = 8.4$ Hz, 1H), 7.57 (t, $J = 7.6$ Hz, 1H), 7.20 (d, $J = 8.8$ Hz, 2H), 5.39 (s, 2H), 3.61 (s,

3H); ^{13}C NMR (100 MHz, DMSO) δ 167.4, 161.7, 152.6, 146.9, 134.9, 131.8, 127.8, 127.6, 126.7, 124.3, 120.7, 115.3, 68.8, 30.3; HRMS-ESI (m/z): $[M + H]^+$ calcd for $C_{17}H_{14}N_2O_4$, 311.1036; found, 311.1023.

2.1.6. N-(3-Fluorophenyl)-4-((3-methyl-4-oxo-3,4-dihydroquinazolin-2-yl)methoxy)benzamide (**4b**)

Compound **6** (310 mg, 1 mmol) and 3-fluorobenzamide (111 mg, 1 mmol) were dissolved in DMF (5 ml), and then HATU (o-(7-aza-1H-benzotriazol-1-yl)- N,N,N' -tetramethyluronium hexafluorophosphate) (380 mg, 1 mmol) was added. After stirred for 30 min, the mixture was added DIEA (N,N -diisopropylethylamine) (129 mg, 1 mmol) and stirred for 12 h at room temperature. The solution was poured into water (20 ml). The final product was filtered and

dried in vacuum to give a white solid. 153 mg; 38% yield; m.p. 196–197 °C; ^1H NMR (400 MHz, DMSO) δ 10.28 (s, 1H), 8.16 (d, $J=8.0$ Hz, 1H), 7.96 (d, $J=8.8$ Hz, 2H), 7.83 (t, $J=7.6$ Hz, 1H), 7.74 (d, $J=12.0$ Hz, 1H), 7.65 (d, $J=8.0$ Hz, 1H), 7.56 (dd, $J=14.0$, 7.6 Hz, 2H), 7.37 (dd, $J=15.6$, 8.0 Hz, 1H), 7.26 (d, $J=8.8$ Hz, 2H), 6.91 (td, $J=8.4$, 2.4 Hz, 1H), 5.42 (s, 2H), 3.63 (s, 3H); ^{13}C NMR (125 MHz, DMSO) δ 152.5, 150.8, 149.4 (d, $J=19.0$ Hz), 148.8, 142.2, 137.5, 133.3 (d, $J=9.0$ Hz), 128.0, 124.6 (d, $J=7.5$ Hz), 124.1, 122.4 (d, $J=15.5$ Hz), 122.1, 121.4, 116.6, 113.1, 112.2, 108.3 (d, $J=16.5$ Hz), 105.9, 105.8, 75.1, 44.3; HRMS-ESI (m/z): $[\text{M} + \text{H}]^+$ calcd for $\text{C}_{23}\text{H}_{18}\text{FN}_3\text{O}_3$, 404.1404; found, 404.1405.

2.1.7. (E)-1-(4-Methoxystyryl)-3-fluorobenzene (8)

1-(Chloromethyl)-4-methoxybenzene (1.56 g, 10 mmol) was dissolved in triethyl phosphate (50 ml), and then tetrabutylammonium bromide (322 mg, 1 mmol) was added. The mixture was stirred at 130 °C under argon for overnight. After evaporated under vacuum, the solution was added to the solution of 3-fluorobenzaldehyde (1.24 g, 10 mmol) in anhydrous THF (50 ml). The mixture was added NaH (600 mg, 15 mmol, 60% in oil) at 0–10 °C and stirred for 12 h at room temperature. The solution was added to water (100 ml) and extracted with EtOAc (100 ml \times 2), and dried over MgSO_4 for 6 h. The crude product was evaporated and purified with flash chromatography using PE/EtOAc = 1/1 as the fluent solvent. The product was dried in vacuum to give a light solid. 980 mg; 43% yield; ^1H NMR (400 MHz, CDCl_3) δ 7.47–7.42 (m, 2H), 7.28 (dd, $J=8.0$, 6.0 Hz, 1H), 7.24–7.16 (m, 2H), 7.05 (d, $J=16.4$ Hz, 1H), 6.94–6.87 (m, 4H), 3.83 (s, 3H). Spectral properties were in accordance with the literature²⁴.

2.1.8. (E)-4-(3-Fluorostyryl)phenol (9)

Compound **8** (1.14 g, 5 mmol) was dissolved in DCM (10 ml), and then 1 mol/l BBr_3 (10 ml) in THF was added at 0–10 °C. The mixture was stirred at room temperature for 6 h. The solution was evaporated under vacuum. The crude product was filtered and purified with recrystallisation from ethanol. The product was dried in vacuum to give a white solid. 770 mg; 72% yield; ^1H NMR (400 MHz, CDCl_3) δ 7.43–7.39 (m, 2H), 7.30 (td, $J=8.0$, 6.0 Hz, 1H), 7.24–7.16 (m, 2H), 7.05 (d, $J=16.4$ Hz, 1H), 6.95–6.89 (m, 2H), 6.86–6.82 (m, 2H), 4.83 (s, 1H). Spectral properties were in accordance with the literature²⁵.

2.1.9. (E)-2-((4-(3-Fluorostyryl)phenoxy)methyl)-3-methylquinazolin-4(3H)-one (4c)

Compound **9** (214 mg, 1 mmol) was dissolved in DMF (5 ml), and then anhydrous K_2CO_3 (152 mg, 1.1 mmol) was added. After stirred for 15 min at room temperature, the mixture was added compound **2** (208 g, 1 mmol) and KI (183 mg, 1.1 mmol). The solution was stirred for the other 2 h, and poured into water (40 ml). The crude product was filtered and purified with recrystallisation from ethanol. The product was dried in vacuum to give a white solid. 181 mg; 47% yield; m.p. 160–162 °C; ^1H NMR (400 MHz, CDCl_3) δ 8.30 (d, $J=8.0$ Hz, 1H), 7.79–7.70 (m, 2H), 7.54–7.45 (m, 3H), 7.29 (dd, $J=8.0$, 6.0 Hz, 1H), 7.20 (dd, $J=20.0$, 9.2 Hz, 2H), 7.05 (dd, $J=12.8$, 6.4 Hz, 3H), 6.93 (dd, $J=9.2$, 7.2 Hz, 2H), 5.21 (s, 2H), 3.75 (s, 3H); ^{13}C NMR (125 MHz, DMSO) δ 151.3, 149.7, 149.5, 146.5, 142.4, 137.6, 132.4 (d, $J=6.5$ Hz), 128.0, 124.8 (d, $J=6.5$ Hz), 124.6, 124.0, 122.8, 122.2 (d, $J=19.5$ Hz), 121.4, 120.7, 118.5, 116.6, 112.7, 111.51 (d, $J=17.0$ Hz), 110.2 (d, $J=17.0$ Hz), 75.4, 44.4; HRMS-ESI (m/z): $[\text{M} + \text{H}]^+$ calcd for $\text{C}_{24}\text{H}_{19}\text{FN}_2\text{O}_2$, 387.1503; found, 387.1499.

2.1.10. 3-Methyl-2-((4-nitrophenoxy)methyl)quinazolin-4(3H)-one (10)

4-Nitrophenol (695 mg, 5 mmol) was dissolved in DMF (20 ml), and then anhydrous K_2CO_3 (759 mg, 5.5 mmol) was added. After stirred for 15 min at room temperature, the mixture was added compound **2** (1.04 g, 5 mmol) and KI (915 mg, 5.5 mmol). The solution was stirred for the other 2 h, and poured into water (80 ml). The crude product was filtered and purified with recrystallisation from ethanol. The product was dried in vacuum to give a yellow solid. 824 mg; 53% yield; m.p. 185–186 °C; ^1H NMR (400 MHz, CDCl_3) δ 8.32 (dd, $J=8.0$, 1.2 Hz, 1H), 8.27–8.23 (m, 2H), 7.81 (ddd, $J=8.4$, 7.2, 1.6 Hz, 1H), 7.74 (dd, $J=8.0$, 0.8 Hz, 1H), 7.56 (ddd, $J=8.0$, 7.2, 1.2 Hz, 1H), 7.23–7.19 (m, 2H), 5.33 (s, 2H), 3.77 (s, 3H); ^{13}C NMR (125 MHz, DMSO) δ 150.9, 149.4, 141.8, 137.5, 133.5, 128.0, 122.3, 122.1, 121.4, 121.0, 116.6, 112.9, 75.0, 44.1; HRMS-ESI (m/z): $[\text{M} + \text{H}]^+$ calcd for $\text{C}_{16}\text{H}_{13}\text{N}_3\text{O}_4$, 312.0978; found, 312.0982.

2.1.11. 2-((4-Aminophenoxy)methyl)-3-methylquinazolin-4(3H)-one (11)

Compound **10** (622 mg, 2 mmol) was dissolved in MeOH (10 ml), and then Pd/C (62 mg, 10%) was added. The mixture was stirred at room temperature under hydrogen atmosphere for overnight. The solution was filtered with celite and the filtration was evaporated under vacuum. The crude product was purified with recrystallisation from MeOH. The product was dried in vacuum to give a light-yellow solid. 405 mg; 72% yield; m.p. 165–166 °C; ^1H NMR (400 MHz, CDCl_3) δ 8.29 (d, $J=8.8$ Hz, 1H), 7.78–7.68 (m, 2H), 7.53–7.48 (m, 1H), 6.90–6.85 (m, 2H), 6.67–6.62 (m, 2H), 5.09 (s, 2H), 3.75 (s, 3H), 3.49 (s, 2H); ^{13}C NMR (125 MHz, DMSO) δ 149.5, 142.8, 139.4, 137.6, 135.2, 128.0, 122.3, 122.1, 121.4, 116.6, 113.4, 112.2, 76.6, 44.6; HRMS-ESI (m/z): $[\text{M} + \text{H}]^+$ calcd for $\text{C}_{16}\text{H}_{15}\text{N}_3\text{O}_2$, 282.1236; found, 282.1241.

2.1.12. 3-Fluoro-N-(4-((3-methyl-4-oxo-3,4-dihydroquinazolin-2-yl)methoxy)phenyl)benzamide (4d)

Compound **11** (281 mg, 1 mmol) and 3-fluorobenzoic acid (140 mg, 1 mmol) were dissolved in DMF (5 ml), and then HATU (o-(7-aza-1H-benzotriazol-1-yl)- N,N,N',N' -tetramethyluronium hexafluorophosphate) (380 mg, 1 mmol) was added. After stirred for 30 min, the mixture was added DIEA (N,N -diisopropylethylamine) (129 mg, 1 mmol) and stirred for 12 h at room temperature. The solution was poured into water (20 ml). The final product was filtered and dried in vacuum to give a white solid. 149 mg; 37% yield; m.p. 228–229 °C; ^1H NMR (400 MHz, DMSO) δ 10.23 (s, 1H), 8.17 (dd, $J=8.0$, 1.2 Hz, 1H), 7.86–7.79 (m, 2H), 7.77–7.73 (m, 1H), 7.71–7.67 (m, 3H), 7.57 (dt, $J=2.0$, 1.6 Hz, 2H), 7.44 (td, $J=8.4$, 2.4 Hz, 1H), 7.15–7.10 (m, 2H), 5.29 (s, 2H), 3.64 (s, 3H); ^{13}C NMR (125 MHz, DMSO) δ 151.4, 150.7, 149.5, 149.2, 143.6, 142.5, 137.6, 130.2 (d, $J=5.5$ Hz), 128.0, 126.7, 124.9 (d, $J=6.5$ Hz), 122.2 (d, $J=17.0$ Hz), 121.4, 119.5, 118.0, 116.6, 115.1 (d, $J=16.5$ Hz), 112.5, 111.9 (d, $J=18.0$ Hz), 75.6, 44.4; HRMS-ESI (m/z): $[\text{M} + \text{Na}]^+$ calcd for $\text{C}_{23}\text{H}_{17}\text{FN}_3\text{NaO}_3$, 426.1224; found, 426.1226.

2.1.13. 3,4-Difluoro-N-(4-((3-methyl-4-oxo-3,4-dihydroquinazolin-2-yl)methoxy)phenyl)benzamide (4e)

Compound **11** (281 mg, 1 mmol) and 3,4-difluorobenzoic acid (158 mg, 1 mmol) were dissolved in DMF (5 ml), and then HATU (o-(7-aza-1H-benzotriazol-1-yl)- N,N,N',N' -tetramethyluronium hexafluorophosphate) (380 mg, 1 mmol) was added. After stirred for 30 min, the mixture was added DIEA (N,N -diisopropylethylamine)

(129 mg, 1 mmol) and stirred for 12 h at room temperature. The solution was poured into water (20 ml). The final product was filtered and dried in vacuum to give a white solid. 139 mg; 33% yield; m.p. 248–249 °C; ¹H NMR (400 MHz, DMSO) δ 10.23 (s, 1H), 8.16 (dd, *J* = 8.0, 1.2 Hz, 1H), 8.05–7.98 (m, 1H), 7.84 (dd, *J* = 12.0, 4.8 Hz, 2H), 7.70–7.55 (m, 5H), 7.13 (d, *J* = 9.2 Hz, 2H), 5.28 (s, 2H), 3.63 (s, 3H); ¹³C NMR (125 MHz, DMSO) δ 152.1, 150.7, 149.5, 143.7, 142.5, 137.6, 128.0, 126.6, 126.2 (d, *J* = 6.0 Hz), 122.2 (d, *J* = 18.0 Hz), 121.4, 120.5 (d, *J* = 2.0 Hz), 118.0, 116.6, 114.6, 114.5, 114.1, 114.0, 112.5, 75.6, 44.4; HRMS-ESI (*m/z*): [M + Na]⁺ calcd for C₂₃H₁₆F₂N₃NaO₃, 444.1130; found, 444.1126.

2.1.14. (E)-3-(3,4-Difluorophenyl)-N-(4-((3-methyl-4-oxo-3,4-dihydroquinazolin-2-yl)methoxy)phenyl)acrylamide (4f)

Compound **11** (281 mg, 1 mmol) and (E)-3-(3,4-difluorophenyl)acrylic acid (184 mg, 1 mmol) were dissolved in DMF (5 ml), and then HATU (o-(7-aza-1H-benzotriazol-1-yl)-N,N,N',N'-tetramethyluronium hexafluorophosphate) (380 mg, 1 mmol) was added. After stirred for 30 min, the mixture was added DIEA (N,N-diisopropylethylamine) (129 mg, 1 mmol) and stirred for 12 h at room temperature. The solution was poured into water (20 ml). The final product was filtered and dried in vacuum to give a white solid. 134 mg; 30% yield; m.p. 235–236 °C; ¹H NMR (400 MHz, DMSO) δ 10.16 (s, 1H), 8.16 (d, *J* = 8.0 Hz, 1H), 7.86–7.82 (m, 1H), 7.75–7.63 (m, 4H), 7.59–7.49 (m, 4H), 7.11 (d, *J* = 9.1 Hz, 2H), 6.78 (d, *J* = 15.7 Hz, 1H), 5.27 (s, 2H), 3.63 (s, 3H); ¹³C NMR (125 MHz, DMSO) δ 150.6, 149.5, 143.4, 142.5, 137.6, 130.5, 128.0, 127.0, 126.6 (d, *J* = 5.0 Hz), 122.3, 122.1, 121.4, 120.2 (d, *J* = 2.5 Hz), 119.4, 118.2, 116.9, 116.6, 114.9 (d, *J* = 14.0 Hz), 113.6 (d, *J* = 14.0 Hz), 113.3, 112.6, 75.7, 44.5; HRMS-ESI (*m/z*): [M + Na]⁺ calcd for C₂₅H₁₈F₂N₃NaO₃, 470.1287; found, 470.1288.

2.1.15. 1-(3-Fluorophenyl)-3-(4-((3-methyl-4-oxo-3,4-dihydroquinazolin-2-yl)methoxy)phenyl)urea (4g)

Compound **11** (281 mg, 1 mmol) was dissolved in anhydrous THF (5 ml), and then 1-fluoro-3-isocyanatobenzene (137 mg, 1 mmol) was added. After stirred for 30 min, the mixture was added DIEA (129 mg, 1 mmol) and stirred for 12 h at room temperature. The solution was poured into water (20 ml). The crude product was purified with recrystallisation from MeOH. The product was dried in vacuum to give a white solid. 142 mg; 34% yield; m.p. 195–196 °C; ¹H NMR (400 MHz, DMSO) δ 9.13 (s, 1H), 8.84 (s, 1H), 8.16 (dd, *J* = 8.0, 1.2 Hz, 1H), 7.87–7.80 (m, 1H), 7.68 (d, *J* = 8.0 Hz, 1H), 7.57 (t, *J* = 7.6 Hz, 1H), 7.48 (dt, *J* = 12.0, 2.4 Hz, 1H), 7.39 (d, *J* = 9.2 Hz, 2H), 7.28 (dd, *J* = 15.2, 8.0 Hz, 1H), 7.12 (dd, *J* = 8.4, 0.8 Hz, 1H), 7.06 (d, *J* = 9.2 Hz, 2H), 6.75 (td, *J* = 8.4, 2.4 Hz, 1H), 5.24 (s, 2H), 3.63 (s, 3H); ¹³C NMR (125 MHz, DMSO) δ 151.1, 149.5 (d, *J* = 10.0 Hz), 142.6, 142.5, 137.6, 134.0 (d, *J* = 9.5 Hz), 128.0, 127.3, 124.6 (d, *J* = 8.0 Hz), 122.3, 122.2, 121.4, 116.6, 116.4, 112.7, 111.4, 106.6 (d, *J* = 17.0 Hz), 104.2, 104.0, 75.8, 44.5; HRMS-ESI (*m/z*): [M + Na]⁺ calcd for C₂₃H₁₈FN₄NaO₃, 441.1333; found, 441.1333.

2.2. In vitro EGFR^{WT}-TK assay

Enzymatic inhibition of synthesised compounds against wild type EGFR tyrosine kinase was determined with enzyme-linked immunosorbent assays (ELISAs) as our previous methods. The recombinant EGFR^{WT}-TK and Antiphosphotyrosine mouse mAb were purchased from PTM Bio. The IC₅₀ value was determined from a sigmoid dose–response curve using Graph-Pad Prism (GraphPad Software, San Diego, CA).

2.3. In vitro activity assay at cell level

2.3.1. Cell culture

A431 (Human epidermoid carcinoma cell line) cell, A549 (Human non-small cell lung cancer cell line) cell, MCF-7 (Human breast adenocarcinoma cell line) cell, and NCI-H1975 (Human non-small cell lung cancer cell line) cell were purchased from the Shanghai Cell Bank of the Chinese Academy of Sciences. NRK-52E (Normal rat kidney cell line) cell was donated by Guizhou Medical University. All cell lines were maintained in RPMI 1640 or DMEM complete medium.

2.3.2. Cytotoxicity evaluation (MTT assay)

In vitro cytotoxicity of compounds **4a–4g** against four cancer cell lines (A431, A549, MCF-7, and NCI-H1975) and normal rat kidney cells (NRK 52E) was determined by MTT assay as our previous report. Gefitinib were used as positive controls. The IC₅₀ value was determined from a sigmoid dose–response curve using Graph-Pad Prism (GraphPad Software, San Diego, CA).

2.3.3. Cell apoptosis analysis

The apoptosis of tumour cells MCF-7 treated by different concentrations of compound **4d**, was measured with Annexin V - FITC/PI apoptosis detection kit (Solarbio, Beijing, China), according to instructions of kit, and detected by BD Accuri C6 flow cytometry (American BD Corporation Shanghai Co. Ltd.).

2.3.4. Cell cycle analysis

The distribution of cell cycle for MCF-7 treated by different concentrations of compound **4d**, was measured with Annexin V - FITC/PI cell cycle detection kit (Solarbio, Beijing, China), according to instructions of kit, and detected by BD Accuri C6 flow cytometry (American BD Corporation Shanghai Co. Ltd.).

2.4. Molecular docking

X-ray crystal structures of EGFR in both “active” (PDB entry 1M17) and “inactive” (PDB entry 4HJO) states were used for identifying candidate binding modes. The possible binding modes of compound **4a–4g**, Gefitinib with EGFR were predicted by molecular docking with Sybyl X-2.0 software from Tripos Inc, St. Louis, MI.

2.5. Admet studies

The absorption, distribution, metabolism, elimination, and toxicity (ADMET) parameters of compounds **4a–4g** and Gefitinib were calculated in and calculated in CHARMM Force Field of Discovery Studio 2.5 Software (Accelrys Inc., San Diego, CA). The data of ADMET included Solubility, Absorption, Cytochrome P450 (CYP2D6), Hepatotoxicity, Plasma protein binding (PPB), Blood brain barrier permeability (BBB), and water partition coefficients for the unionised species (AlogP98)²⁶.

3. Results and discussions

3.1. Chemistry

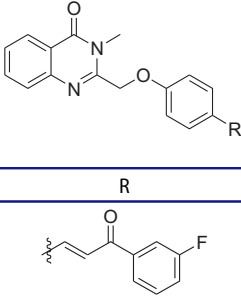
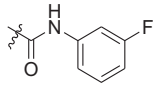
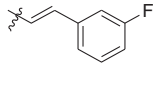
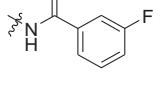
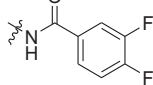
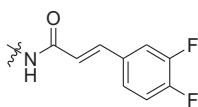
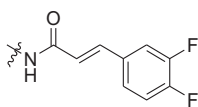
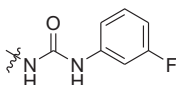
All target compounds (**4a–4g**) were synthesised and confirmed based on ¹H-NMR, ¹³C-NMR and HRMS. The synthetic route was shown in Scheme 1. At first, compound **2** and **3** were prepared

under the described conditions in literature²³. And then, compound **3** experienced in aldol-condensation with 3-fluorophenylethanone to give the product **4a**. Subsequently, compound **3** reacted with ethyl 4-hydroxybenzoate under the condition of $K_2CO_3/KI/DMF$ to give the compound **5** with 64% yield. After hydrolysis in the presence of NaOH, compound **6** was obtained with 58% yield and formed amide **4b** with 3-fluorobenzaniline. Next, compound **9** was prepared with the reported method and reacted with compound **2** to give styrylquinazolinone **4c**. At last, treatment **2** with 4-nitrophenol and reduce the nitro-group to give the intermediate **11**. Compound **11** reacted with corresponding acid or isocyanate to obtain the final targets **4d–4g**. The synthetic details were described in experimental section and the spectra can be found in the [supplementary material](#).

3.2. In vitro EGFR kinase inhibitory activity and antitumor activity of target quinazolinone derivatives

With the compounds **4a–4g** in hand, the activity against EGFR^{WT}-TK was tested with ELISA assay²⁷. As shown in [Table 1](#), when the enamine bond of compound **A** (IC_{50} of 0.047 μM) was substituted

Table 1. IC_{50} values for EGFR^{WT}-TK.

Entry	Comp.	R	EGFR ^{WT} -TK IC_{50} (μM)
1	4a		2.71 ± 0.22
2	4b		1.63 ± 0.15
3	4c		0.20 ± 0.041
4	4d		0.053 ± 0.008
5	4e		0.061 ± 0.007
6	4f		0.38 ± 0.075
7	4g		0.71 ± 0.093
8	A		0.047 ± 0.004
Gefitinib			0.0061 ± 0.0003

^aThe values are mean ± SD of three replicates.

with ketene group ([Table 1, 4a](#)), vinyl group ([Table 1, 4c](#)), and amide bond ([Table 1, 4b](#) and [4d](#)), the IC_{50} values of compounds **4a–d** to EGFR^{WT}-TK were 2.71 μM , 0.2 μM , 1.63 μM and 0.053, respectively. Fortunately, compound **4d** reached in the similar activity with compound **A**. Compared to **4d**, 3,4-difluoro substitution on the phenyl ring ([Table 1, 4e](#)) decreased the activity. Meanwhile, the extended amide bond ([Table 1, 4f](#)) and urea bond ([Table 1, 4g](#)) also significantly weaken the activity.

To investigate the anticancer activity of the synthesised compounds, four EGFR over-expressed human tumour cell lines derived from human epidermoid cancer (A431), non-small cell lung cancer (A549), breast cancer (MCF-7), and non-small cell lung cancer (NCI-H1975) were used to evaluate the antiproliferative activities by methyl thiazolyl tetrazolium colorimetric assay (MTT). Gefitinib, a clinical drug targeted EGFR was employed as positive control. As shown in [Table 2](#), against A431 cells compounds **4d** and **4e** (IC_{50} values of 3.48 μM and 3.53 μM) were more potent than Gefitinib (4.45 μM), while compounds **4a, 4b, 4c, 4f**, and **4g** (IC_{50} values of 9.32, 8.72, 6.79, 8.76 μM and 8.34 μM , respectively). Against A549 cells compounds **4c–4f** (with IC_{50} values of 4.26, 2.55, 2.69, 8.46, and 7.31 μM , respectively) were more potent than Gefitinib (8.47 μM). Against NCI-H1975 cells compounds **4c–4f** showed higher inhibitor activities than Gefitinib. Against MCF-7 cells compounds **4d–4f** (with IC_{50} values of 0.87, 0.96, and 2.84 μM , respectively) were more efficient than Gefitinib (5.89 μM).

Based on the result of EGFR^{WT}-TK and four tumour cell assays, we found that the similar structure–activity relationship (SAR) was observed in cell lines and EGFR-TKs. The amide group (**4d** and **4e**) instead of enamine was more potent than the ketene group (**4a**), vinyl group (**4c**), urea group (**4g**) and other groups (**4b** and **4f**). Besides, compound **A** showed lower inhibitor activities against four tumour cell lines than the compounds **4a–4g**. The reason may be due to the lower stability of compound **A** in cells. Generally, compound **4d** was the best in the synthesised compounds and particularly showed much higher inhibitor activities than Gefitinib against four tumour cells. These data indicate that **4d** was worth to further investigation.

3.3. In vitro cytotoxicity of 3-methyl quinazolinone derivatives on normal cells

The cytotoxicity study of compounds **4a–4g** was first evaluated by MTT colorimetric assays to normal rat kidney cell line (NRK-52E) at different concentrations. There was no inhibition of all compounds including Gefitinib at 10 μM . Therefore, the concentration was accelerated to 100 μM . As shown in [Figure 2](#), all compounds were similar with Gefitinib and not more than 25% against NRK-52E at 100 μM . This indicate that the synthesised compounds **4a–4g** were low cytotoxicity and potent for development for drugs.

3.4. Effects of compound 4d on cell apoptosis of MCF-7 cell line

Apoptosis of tumour cell is the basic mechanism of tissue homeostasis, which is regarded as the efficient method to eliminate the excess cells²⁸. Most of the anti-cancer drugs perform as a well inducing apoptosis for cancer cells²⁹. As shown in [Figure 3](#), compound **4d** was used to investigate the mechanism of inhibition of MCF-7 cell proliferation. Flow cytometry analysis of MCF-7 treated with **4d** at 5 and 10 μM for 48 h demonstrated a prominent increase in apoptotic cells with a dose-dependent fashion. The trend of compound **4d** showed that early apoptosis rate was priority over late apoptosis. Compared compound **4d** with Gefitinib,

Table 2. IC₅₀ values for human cancer cell lines^a.

Comp.	R	IC ₅₀ (μM)			
		A431	A549	MCF-7	NCI-H1975
4a		9.32 ± 0.57	8.63 ± 0.41	10.58 ± 1.03	13.68 ± 1.61
4b		8.72 ± 0.46	9.08 ± 0.69	9.64 ± 0.88	12.87 ± 1.44
4c		6.79 ± 0.72	4.26 ± 0.57	6.04 ± 0.73	6.44 ± 0.85
4d		3.48 ± 0.49	2.55 ± 0.26	0.87 ± 0.14	6.42 ± 0.47
4e		3.53 ± 0.34	2.69 ± 0.32	0.96 ± 0.21	7.18 ± 0.49
4f		8.76 ± 0.74	8.46 ± 0.67	2.84 ± 0.22	9.33 ± 0.78
4g		8.35 ± 0.46	7.31 ± 0.59	10.74 ± 2.07	10.19 ± 1.03
A		17.71 ± 2.08	17.86 ± 2.11	14.09 ± 1.85	19.18 ± 3.02
Gefitinib		4.45 ± 0.25	8.47 ± 1.06	5.89 ± 0.72	9.71 ± 1.96

^aThe values are mean ± SD of three replicates.

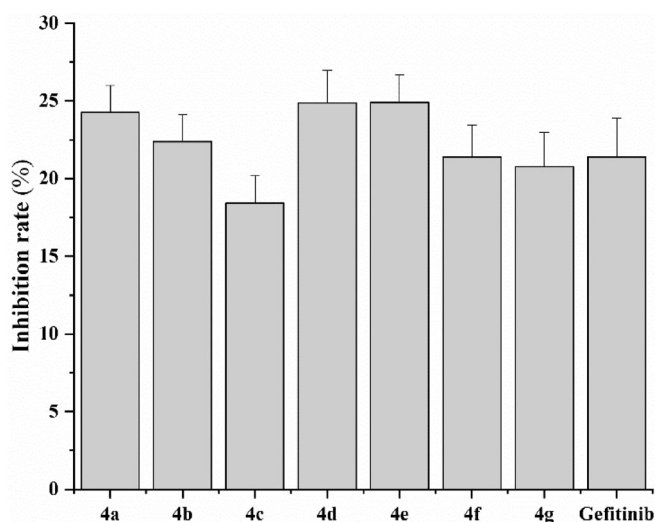


Figure 2. *In vitro* cytotoxicity of compounds **4a-g** and **Gefitinib** on NRK-52E cell.

the results in **Figure 3(B)** showed that **4d** significantly performed better ability to induce early apoptosis at the same concentration. Particularly, the ratio of apoptotic cells for compound **4d** reached 28.14% (early) and 41.36% (late) even at 5 μM.

3.5. Effects of compound **4d** on cell cycle of MCF-7 cell line

Next, we wished to determine whether **4d**-induced decrease of EGFR phosphorylation would result in cell cycle arrest in MCF-7 cell lines, compared with Gefitinib. As shown in **Figure 4**, cell cycle analysis was tested in flow cytometry. MCF-7 cell lines were treated with compound **4d** at 5 and 10 μM. Against MCF-7 cells at 5 μM, the control consisted of 6.06% G2 phase cells, compound **4d** increased to 10.38% and Gefitinib also reached to 11.58%. However, at 10 μM of tested samples, G2/M phase decreased and S phase increased, this might be that compound **4d** and Gefitinib undergo significant apoptosis. These results indicate that compound **4d** and Gefitinib could arrest MCF-7 cells in G2/M phase at the appropriate concentration.

3.6. Molecular docking studies

To explain the structural activity relationship of EGFR with our compounds, the possible binding modes were performed in molecular docking studies³⁰. Former researches showed that the "active" or "inactive" state of EGFR-TK has different preference of ligand binding profile, so X-ray crystal structures of EGFR in both "active" (PDB entry 1M17) and "inactive" (PDB entry 4HJO) states were used for identifying candidate binding modes³¹.

As shown in **Tables S1** and **S2**, the predicted score of all compounds **4a-4g** with inactive state of EGFR (PDB: 4HJO) is much

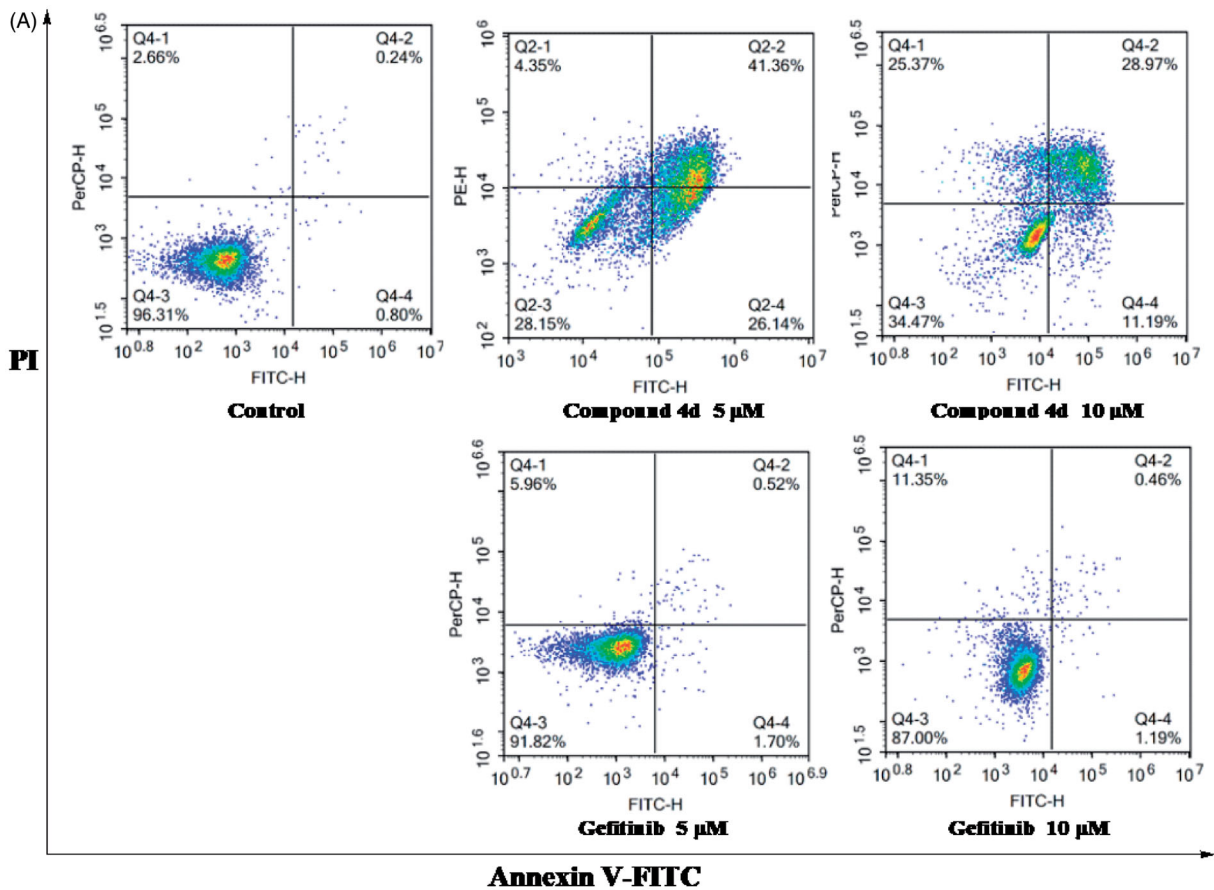


Figure 3. Compound **4d** induced cell apoptosis in Annexin V-FITC assay. (A) Density plot were obtained by flow cytometry, Gefitinib was used as reference drug. (B) Total apoptotic cells (%) at various concentrations of **4d** and Gefitinib.

higher than the score of active state of EGFR (PDB: 1M7), which suggests that the compounds **4a–4g** are likely to bind with EGFR in inactive state. By contrast, the predicted binding model for Gefitinib in two states are similar, which is consistent with our previous work. More interestingly, as shown in Figure 5(A,C), all

the compounds **4a–4g** were employed in the same binding configuration with EGFR active state or inactive state. Take compound **4d** as example, in Figure 5(B) for active state, simply formed one hydrogen bond with Met769 during the docking situation. However, in Figure 5(D) for inactive state, quinazolinone ring of

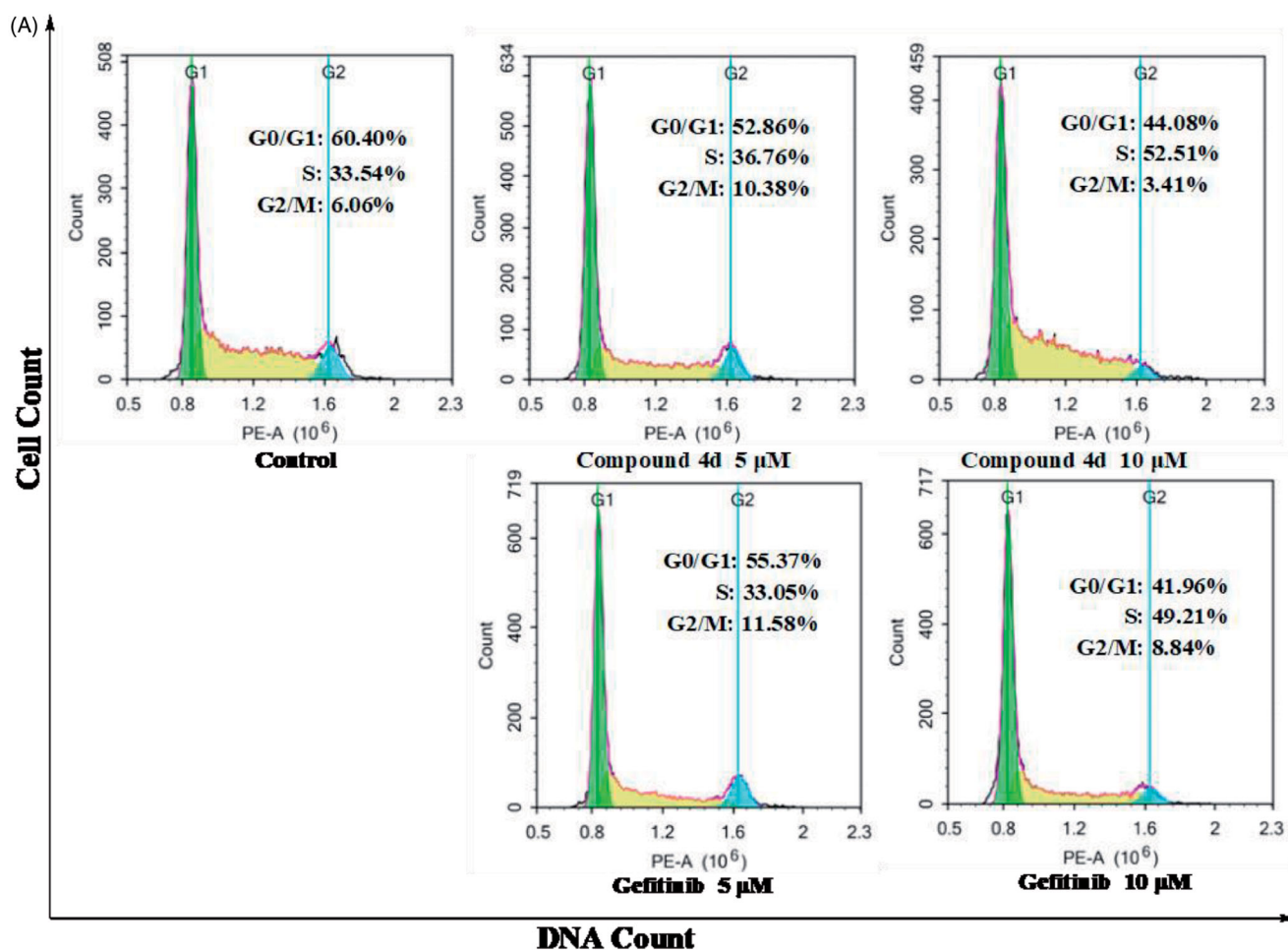


Figure 4. Cell cycle distribution of compound **4d** and Gefitinib against MCF-7 was studied by flow cytometry. (A) Profiles were obtained by FACS. The percentages for different phases of cell cycle were illustrated in the histogram. (B) MCF-7 cells were cultured in the presence of different concentrations of **4d** (5 μM and 10 μM) or Gefitinib (5 μM and 10 μM) for 48 h, harvested, fixed, and labelled with PI, then analysed by FACS. Percentage of cells in G0/G1, S and G2/M phases are indicated.

compound **4d** formed stable hydrogen bonds with Lys692 and Lys704. Meanwhile, amide group and fluorine atom of **4d** also formed hydrogen bonds with Thr766, Thr830, and Lys721 respectively. These results indicate that the synthesised compounds **4a-4g** are particularly likely to be potential EGFR inhibitors against inactive state.

3.7. Admet and stability studies

The ADMET are essential aspects for drug candidates³². Computer aided ADMET studies have been employed in the early stage of drug discovery. Therefore, the ADMET properties of compounds **4a-4g** were calculated through Discovery Studio 2.5 software

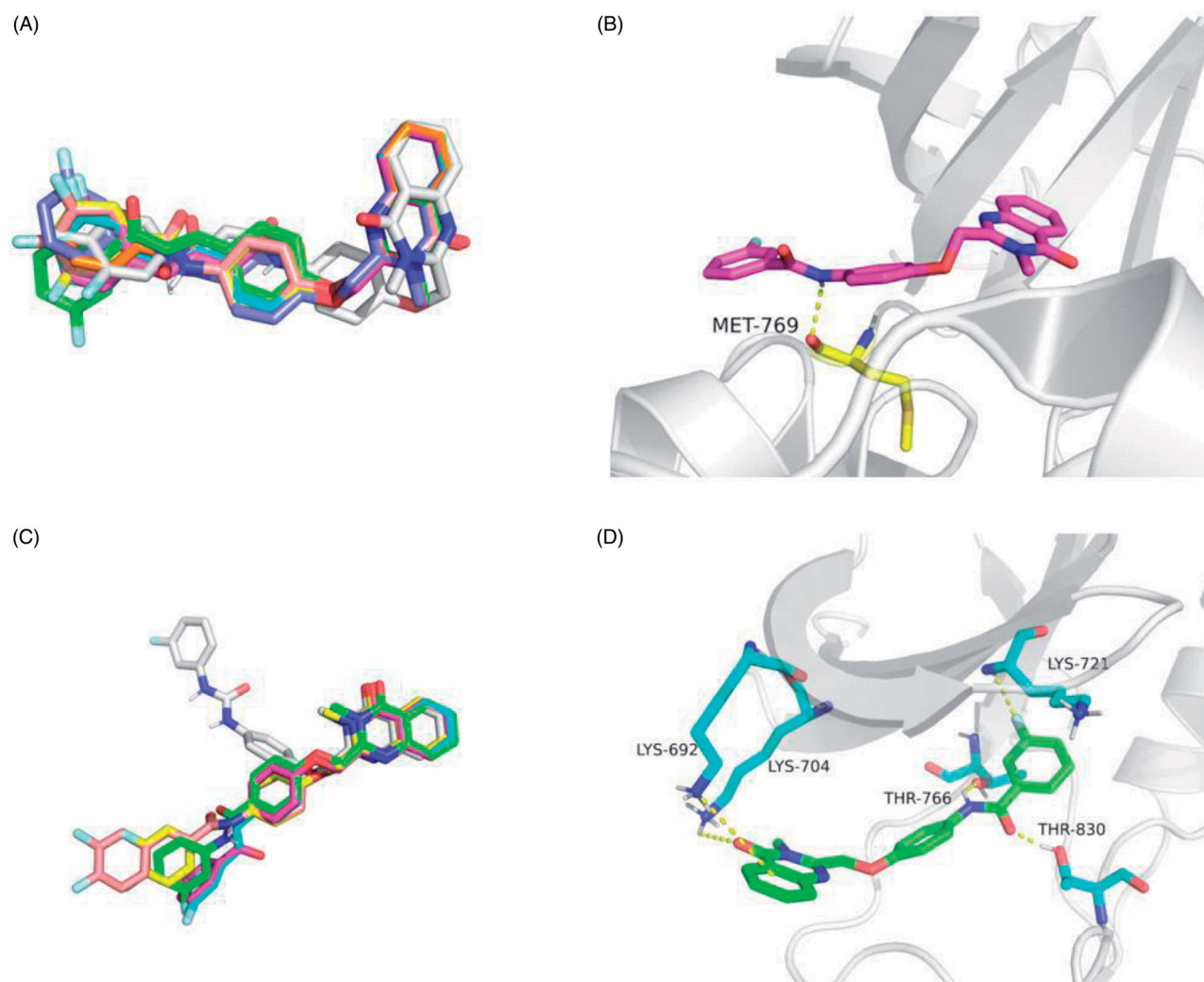


Figure 5. Docking structures of compounds **4a-4g**. (A) Different binding configurations of compounds **4a-4g** with EGFR (PDB: 1M17). (B) The 3D model of compound **4d** bound to EGFR (PDB: 1M17). (C) Different binding configurations of compounds **4a-4g** with EGFR (PDB: 4HJO). (D) The 3D model of compound **4d** bound to EGFR (PDB: 4HJO).

Table 3. ADMET properties of compounds **4a-g**.

Comp.	Solubility	Absorption	CYP2D6	Hepatotoxicity	PPB	BBB	AlogP98
4a	2	0	0	1	2	1	4.61
4b	2	0	1	1	2	2	3.53
4c	2	0	1	1	2	1	4.73
4d	2	0	1	1	2	2	3.52
4e	2	0	1	1	2	2	3.73
4f	2	0	0	1	2	1	4.20
4g	2	0	0	1	2	2	3.63
Gefitinib	2	0	1	0	1	1	4.20

(Accelrys Inc., San Diego, CA). As shown in Table 3, the levels of solubility and absorption were the same with compounds **4a-4g** and Gefitinib. CYP2D6 is non-inhibitor of cytochrome P450 enzyme for predicting drug toxicity. The compounds **4a**, **4f** and **4g** were less toxic than Gefitinib, and the others were similar with Gefitinib. Meanwhile, the calculated log *p* values of compound **4b**, **4d**, **4e** and **4g** were less than Gefitinib (4.20). Particularly, compound **4d** reached the lowest log *p* (3.52) and performed highly oral bioavailability. These data are consistent with the structure-activity relationships.

At last, we investigated the stability of compound **4d** in mice plasma. The results exhibited that compound **4d** was stable with purity higher than 98% after incubation with Sprague Dawley (SD)

mice plasma (Figure S2). All the data suggest that compound **4d** was a good candidate for developing new anti-cancer drug.

4. Conclusions

To solve the issues of metabolic stability in our previous research of EGFR inhibitors, seven 3-methylquinazolinone derivatives were designed and synthesised. After evaluated activities of these compounds in enzyme and cell level, we found that compounds **4d** and **4e** were performed well antiproliferative activities. Furthermore, the best compound **4d** displayed IC₅₀ value of 53 nM against EGFR^{wt}-TK activity and IC₅₀ value of 0.87 μM against MCF-7 cells. Analysis of apoptosis and cell cycle for MCF-7 cells

indicate that compound **4d** could induce apoptosis and arrest in G2/M phase at tested concentration. At last, molecular docking, ADMET, and stability studies suggested that compound **4d** was closely formed hydrogen bonds with EGFR^{wt}-TK and potential to develop new anti-cancer drug.

Disclosure statement

No potential conflict of interest was reported by the author(s).

Funding

This work was financially supported by GZU (Guizhou University) Found for Newly Enrolled Talent ([2019]15), GZU (Guizhou University) Found for Cultivation ([2019]65), and the State Key Laboratory of Functions and Applications of Medicinal Plants, Guizhou Medical University [Grant number FAMP202005K]; Guizhou Science and Technology Platform Talents [QKHRCPT [2019]5106].

ORCID

Guochen Bao  <http://orcid.org/0000-0001-5103-5009>

Longjia Yan  <http://orcid.org/0000-0003-3703-6704>

References

1. Ayati A, Moghimi S, Salarinejad S, et al. A review on progression of epidermal growth factor receptor (EGFR) inhibitors as an efficient approach in cancer targeted therapy. *Bioorg Chem* 2020;99:103811.
2. Roskoski R. Jr., Properties of FDA-approved small molecule protein kinase inhibitors: a 2020 update. *Pharmacol Res* 2020;152:104609.
3. Sigismund S, Avanzato D, Lanzetti L. Emerging functions of the EGFR in cancer. *Mol Oncol* 2018;12:3–20.
4. Xu X, Mao L, Xu W, et al. AC0010, an irreversible EGFR inhibitor selectively targeting mutated EGFR and overcoming T790M-induced resistance in animal models and lung cancer patients. *Mol Cancer Ther* 2016;15:2586–97.
5. Lu X, Yu L, Zhang Z, et al. Targeting EGFR(L858R/T790M) and EGFR(L858R/T790M/C797S) resistance mutations in NSCLC: current developments in medicinal chemistry. *Med Res Rev* 2018;38:1550–81.
6. Lee DH. Treatments for EGFR-mutant non-small cell lung cancer (NSCLC): the road to a success, paved with failures. *Pharmacol Ther* 2017;174:1–21.
7. Jia Y, Yun CH, Park E, et al. Overcoming EGFR(T790M) and EGFR(C797S) resistance with mutant-selective allosteric inhibitors. *Nature* 2016;534:129–32.
8. Mhaske SB, Argade NP. The chemistry of recently isolated naturally occurring quinazolinone alkaloids. *Tetrahedron* 2006;62:9787–826.
9. Auti PS, George G, Paul AT. Recent advances in the pharmacological diversification of quinazoline/quinazolinone hybrids. *RSC Adv* 2020;10:41353–92.
10. Shang XF, Morris-Natschke SL, Yang GZ, et al. Biologically active quinoline and quinazoline alkaloids part II. *Med Res Rev* 2018;38:1614–60.
11. Shang XF, Morris-Natschke SL, Liu YQ, et al. Biologically active quinoline and quinazolinone alkaloids part I. *Med Res Rev* 2018;38:775–828.
12. Zayed MF, Rateb HS, Ahmed S, et al. Quinazolinone-amino acid hybrids as dual inhibitors of EGFR kinase and tubulin polymerization. *Molecules* 2018;23:1699–716.
13. Kong X-F, Guo X-Y, Gu Z-Y, et al. Silver(i)-catalyzed selective hydroalkoxylation of C2-alkynyl quinazolinones to synthesize quinazolinone-fused eight-membered N,O-heterocycles. *Org Chem Front* 2020;7:2055–62.
14. Patel HM, Pawara R, Ansari A, et al. Design and synthesis of quinazolinones as EGFR inhibitors to overcome EGFR resistance obstacle. *Bioorg Med Chem* 2017;25:2713–23.
15. Ghorab MM, Abdel-Kader MS, Alqahtani AS, et al. Synthesis of some quinazolinones inspired from the natural alkaloid L-norephedrine as EGFR inhibitors and radiosensitizers. *J Enzyme Inhib Med Chem* 2021;36:218–37.
16. Yan L, Che X, Bai X, et al. Syntheses of novel diaryl[d,f][1,3]diazepines via one-pot Suzuki coupling followed by direct ring closure with carboxylic acids. *Mol Divers* 2012;16:489–501.
17. Yan L, Wang H, Chen Y, et al. Synthesis and structure-activity relationship study of diaryl[d,f][1,3]diazepines as potential anti-cancer agents. *Mol Divers* 2018;22:323–33.
18. Yan L, Li Y, Deng M, et al. Design, synthesis and biological activities of compounds containing 1,3,4-oxadiazole or 1,3,4-thiadiazole. *Chin J Org Chem* 2020;40:731–9.
19. Yan L, Le Y, Chen D, et al. Synthesis and evaluation of diaminopyrimidine derivatives as dual inhibitors of EGFR and SRC for antitumor treatment. *Heterocycles* 2020;100:418–28.
20. Yan L, Deng M, Chen A, et al. Synthesis of N-pyrimidin[1,3,4]oxadiazoles and N-pyrimidin[1,3,4]-thiadiazoles from 1,3,4-oxadiazol-2-amines and 1,3,4-thiadiazol-2-amines via Pd-catalyzed heteroarylation. *Tetrahedron Lett* 2019;60:1359–62.
21. Le Y, Zhang Y, Wang Q, et al. Microwave-assisted synthesis of phenylpyrimidine derivatives via Suzuki-Miyaura reactions in water. *Tetrahedron Lett* 2021;68:152903.
22. Le Y, Gan Y, Fu Y, et al. Design, synthesis and in vitro biological evaluation of quinazolinone derivatives as EGFR inhibitors for antitumor treatment. *J Enzyme Inhib Med Chem* 2020;35:555–64.
23. Shao L-H, Fan S-L, Meng Y-F, et al. Design, synthesis, biological activities and 3D-QSAR studies of quinazolinone derivatives containing hydrazone structural units. *New J Chem* 2021;45:4626–31.
24. Altarejos J, Sucunza D, Vaquero JJ, et al. Practical solvent-free microwave-assisted hydroboration of alkynes. *Eur J Org Chem* 2020;2020:3024–9.
25. Kuramochi T, Kakefuda A, Yamada H, et al. Synthesis and structure-activity relationships of phenoxy pyridine derivatives as novel inhibitors of the sodium-calcium exchanger. *Bioorg Med Chem* 2004;12:5039–56.
26. Li Y, Yan L, Cai J, et al. Development of novel theranostic agents for in vivo amyloid imaging and protective effects on human neuroblastoma cells. *Eur J Med Chem* 2019;181:111585.
27. Zhang Y, Chen L, Xu H, et al. 6,7-Dimorpholinoalkoxy quinazolinone derivatives as potent EGFR inhibitors with enhanced antiproliferative activities against tumor cells. *Eur J Med Chem* 2018;147:77–89.

28. D'Arcy MS. Cell death: a review of the major forms of apoptosis, necrosis and autophagy. *Cell Biol Int* 2019;43: 582–92.
29. Xie Z, Wu K, Wang Y, et al. Discovery of 4,6-pyrimidinediamine derivatives as novel dual EGFR/FGFR inhibitors aimed EGFR/FGFR1-positive NSCLC. *Eur J Med Chem* 2020;187:111943.
30. Zhang Y, Chen L, Li X, et al. Novel 4-arylaminoquinazolines bearing N,N-diethyl(aminoethyl)amino moiety with antitumour activity as EGFR(wt)-TK inhibitor. *J Enzyme Inhib Med Chem* 2019;34:1668–77.
31. Park JH, Liu Y, Lemmon MA, et al. Erlotinib binds both inactive and active conformations of the EGFR tyrosine kinase domain. *Biochem J* 2012;448:417–23.
32. Jia CY, Li JY, Hao GF, et al. A drug-likeness toolbox facilitates ADMET study in drug discovery. *Drug Discov Today* 2020;25: 248–58.